

Single-channel currents of a peptide-gated sodium channel expressed in *Xenopus* oocytes

Aslbek B. Zhainazarov* and Glen A. Cottrell†

*The Whitney Laboratory, University of Florida, St Augustine, FL 32086-8623, USA and †School of Biomedical Sciences, University of St Andrews, Fife KY16 9TS, UK

(Received 22 April 1998; accepted after revision 10 August 1998)

1. Single-channel recordings were made from outside-out membrane patches of *Xenopus* oocytes injected with the cDNA clone FaNaCh, which encodes a peptide-gated Na⁺ channel from *Helix aspersa*.
2. The natural peptides FMRFamide and FLRFamide only activated unitary currents in oocytes injected with FaNaCh; the EC₅₀ values were 1.8 and 11.7 μM, respectively.
3. The slope conductance of the channel was 9.2 pS for both peptides.
4. With FMRFamide, the open probability (P_o) of the channel was 0.06 at 0.3 μM and 0.76 at 30 μM, whereas for FLRFamide the open probability increased from 0.04 at 1.8 μM to 0.49 at 50 μM. The Hill coefficient was greater than 1 for both peptides.
5. High concentrations of each peptide evoked very fast flickering between open and closed states which led to decreased unitary current amplitude.
6. At low doses, brief single openings and bursts of longer openings occurred. With higher doses, the occurrence of the brief openings declined and the number of longer openings increased; the duration of the longer openings was shorter with FLRFamide than with FMRFamide.
7. For each peptide, frequency distribution histograms of open events were best fitted by the sum of two exponential components, suggesting the existence of two open states of the channel. Closed events were fitted by the sum of three components, suggesting the existence of three closed states.
8. The data were analysed according to a five-state model in which the brief openings correspond to a single liganded open form of the channel and the longer openings to a doubly liganded open form. According to this interpretation, the greater whole-cell response observed with FMRFamide than with FLRFamide results mostly from a slower closing rate constant for the longer (doubly liganded) channel openings.

The neuropeptide Phe-Met-Arg-Phe-NH₂ (FMRFamide) occurs in the ganglia of molluscs (Greenberg & Price, 1992). It is the most abundant of several chemically related peptides. In the snail *Helix aspersa* the precursor of FMRFamide also gives rise to Phe-Leu-Arg-Phe-NH₂ (FLRFamide) and pyro-Glu-Phe-Tyr-Arg-Phe-NH₂ (pQFYRFamide) (Lutz *et al.* 1992; Price *et al.* 1996).

FMRFamide exerts many different ionic responses in molluscan neurones (see e.g. Cottrell *et al.* 1984; Colombaioni *et al.* 1985), some of which are also activated by the other related endogenous peptides (Cottrell & Davies, 1987). Most responses are slow. One response, however, is fast and is evoked only by FMRFamide and FLRFamide. It results from the direct activation of a Na⁺ current that is blocked by amiloride (Green *et al.* 1994). A cDNA clone (FaNaCh) has been identified in *Helix aspersa* that encodes a FMRFamide-

activated Na⁺ channel. FaNaCh, expressed in *Xenopus* oocytes, shows similar properties to the neuronal channel (Lingueglia *et al.* 1995). Although the peptide FLRFamide activates the heterologously expressed channel as well as the neuronal channel, it has a lower apparent affinity than FMRFamide and produces a smaller maximum response (Cottrell, 1997).

The FMRFamide-gated channel is unusual not only because it is gated by a peptide, but also because it is selective for Na⁺ ions. The cloned sequence FaNaCh shows similarity in sequence to epithelial amiloride-sensitive channels (Lingueglia *et al.* 1993; Canessa *et al.* 1993, 1994), to the degenerins of *Caenorhabditis elegans* (Driscoll & Chalfie, 1992; Huang & Chalfie, 1994) and to the recently cloned proton-gated channels of mammalian neurones (Waldmann *et al.* 1997a,b).

Here we have investigated the effects of different concentrations of FMRFamide and FLRFamide on single-channel activity of the clone FaNaCh expressed in *Xenopus* oocytes. The study was made in order to learn more about the properties of this unusual ligand-gated channel and to investigate the basis for the higher apparent affinity and greater maximum response of FMRFamide than of FLRFamide.

METHODS

Preparation of cRNA

cRNA was synthesized from the clone p-BSK-SP6-Globin-FaNaCh, kindly supplied by Drs M. Lazdunski and E. Lingueglia. Plasmid DNA was isolated using Wizard Minipreps (Promega, Madison, WI, USA) and linearized with *NotI* (New England Biolabs, Beverly, MA, USA). The cut plasmid DNA was purified by incubating with proteinase K ($100 \mu\text{g ml}^{-1}$ in 0.5% SDS) at 50°C for 1 h, followed by phenol-chloroform extraction and ethanol precipitation. Transcription was achieved using a T7 mMessage mMachine Kit (Ambion, Austin, TX, USA) and the yield of cDNA assessed, after electrophoresis on 1.1% agarose gel, by comparison with known amounts of marker RNA. Samples of RNA used for electrophoresis were denatured with glyoxal and DMSO.

Preparation and injection of *Xenopus* oocytes

Xenopus laevis were obtained from a commercial supplier (Xenopus I, The Northside, Ann Arbor, MI, USA) and maintained in the laboratory in running water on a diet of frog chow (Nasco), plus diced beef liver once a week.

Defolliculated stage VI oocytes were prepared for injection by treating fragments of ovary with collagenase in calcium-free medium. Segments of ovary were removed from animals anaesthetized with 1 g l^{-1} MS-222 and kept cool during the operation by placing on ice, in accordance with the local approved procedures (Institutional Animal Care and Use Committee of the University of Florida; at the end of the experiment animals were killed with an overdose of anaesthetic). After thoroughly rinsing with calcium-containing medium, released oocytes were selected and checked microscopically for complete removal of follicles; those in clumps were manually defolliculated. Samples (0.5–5 ng) of synthesized cRNA were injected into the cytoplasm of the oocytes, which were then maintained in an incubator at 19°C for 1–12 days before making recordings. Control oocytes were uninjected or injected with water. Before patching, oocytes were placed in hyperosmotic solution (see below for composition) and the vitelline membrane removed manually with fine forceps under a binocular microscope. Oocytes were then transferred to physiological

solution in a 35 mm diameter culture dish mounted on the stage of an inverted microscope (Axiovert 100, Carl Zeiss).

Electrical recording

Outside-out patch recordings were made as described by Hamill *et al.* (1981). Pipettes were pulled from borosilicate glass (BF150-86-10, Sutter Instrument Co.) using a Flaming–Brown micropipette puller (P-87, Sutter Instrument Co.) and fire-polished to a final tip diameter of less than $1 \mu\text{m}$. Pipettes, filled with patch pipette solution (see below for composition), had resistances of 7–10 M Ω ; they easily formed seals on oocyte membrane with resistances of 10–20 G Ω . Single-channel currents were recorded with an Axopatch 200A amplifier (Axon Instruments) using an A/D–D/A interface (TL-1, Axon Instruments) and pCLAMP 6.0 software (Axon Instruments). The recordings were low-pass filtered at 2 kHz (–3 dB; 4-pole Bessel filter) and digitized at 20 kHz. Data were stored on a computer hard disk for later analysis. The recordings were referenced to a Ag–AgCl wire electrode connected to the bath (physiological) solution through a 3 M KCl–agar bridge. All experiments were carried out at room temperature (20 – 22°C).

Solutions

Hyperosmotic solution used to remove the vitelline membrane consisted of (mM): 200 potassium acetate, 20 KCl, 1 MgCl₂, 10 EGTA, 10 Hepes, adjusted to pH 7.4 with KOH.

The physiological solution used in the recording bath contained (mM): 140 NaCl, 1 MgCl₂, 1 CaCl₂, 10 Hepes, adjusted to pH 7.4 with NaOH.

Patch pipettes were filled with ionic solution containing (mM): 140 KF, 1 NaCl, 2 MgCl₂, 5 EGTA, 10 Hepes, adjusted to pH 7.4 with KOH.

Application of peptide solutions

A rotatory perfusion system (RSC-100, Biologic, France) was used to apply different peptide solutions to isolated membrane patches, from up to nine different reservoirs. After forming the outside-out membrane patch in physiological solution, the patch pipette was moved quickly in front of first tube of the perfusion system. Physiological solution continuously flowed from the tube ($100 \mu\text{m}$ inner diameter) and completely engulfed the membrane patch. The remaining eight tubes contained physiological solution with various concentrations of peptides appropriate to the particular experiment. Rapidly moving the tubes in front of the stationary patch pipette allowed solutions to be changed in 10 ms.

Chemicals

All chemicals were purchased from Fisher Scientific except for FMRFamide, FLRFamide and collagenase (Type II), which were obtained from Sigma.

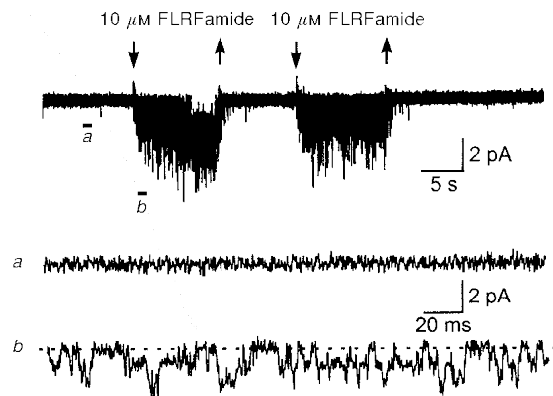


Figure 1. Response of an outside-out patch to application of $10 \mu\text{M}$ FLRFamide

FLRFamide evoked inward single-channel currents throughout the periods of application. Arrows above the current trace show when the peptide was applied. The patch contained several peptide-gated channels. The difference in the current traces before (*a*) and during (*b*) application are shown on an expanded time scale. Channel openings are downwards. The baseline is shown by the dashed line. The membrane potential was -80 mV and the recording was low-pass filtered at 1 kHz (–3 dB).

Data analysis

An idealized recording of the durations and amplitudes of detectable events of the single-channel data was generated using the half-amplitude threshold method (Colquhoun & Sigworth, 1995). Amplitude histograms were binned into equally spaced bins and fitted with the sum of two Gaussian components, using the method of least-squares minimization. Histograms of the distributions of dwell times were plotted as the logarithm of the dwell-time duration, with a square root transformation of the ordinate, and fitted with the sum of several exponential components by using the Levenberg–Marquardt method of least-squares minimization. A fixed time resolution of $90 \mu\text{s}$ was imposed for both open and closed times. A burst of openings was defined as a group of openings separated by closed times shorter than a critical time interval, t_{crit} (Colquhoun & Sigworth, 1995). The value of t_{crit} was calculated so that the number of long closed times (third component in all closed

time distributions) that were misclassified as occurring within bursts was equal to the number of short closed times (second component in all closed time distributions) that were misclassified as occurring between bursts (Colquhoun & Sakmann, 1985; Colquhoun & Sigworth, 1995). The resulting non-linear equation was solved numerically using the bisection method (Press *et al.* 1992) and our own software composed in Basic language (QuickBasic, Microsoft). Unless noted otherwise, results are expressed as the sample mean \pm S.D. of N observations.

RESULTS

Both FMRFamide and FLRFamide evoked single-channel activity in oocytes injected with FaNaCh cRNA, but not in uninjected or water-injected oocytes. An example of peptide-evoked unitary currents is shown in Fig. 1, where

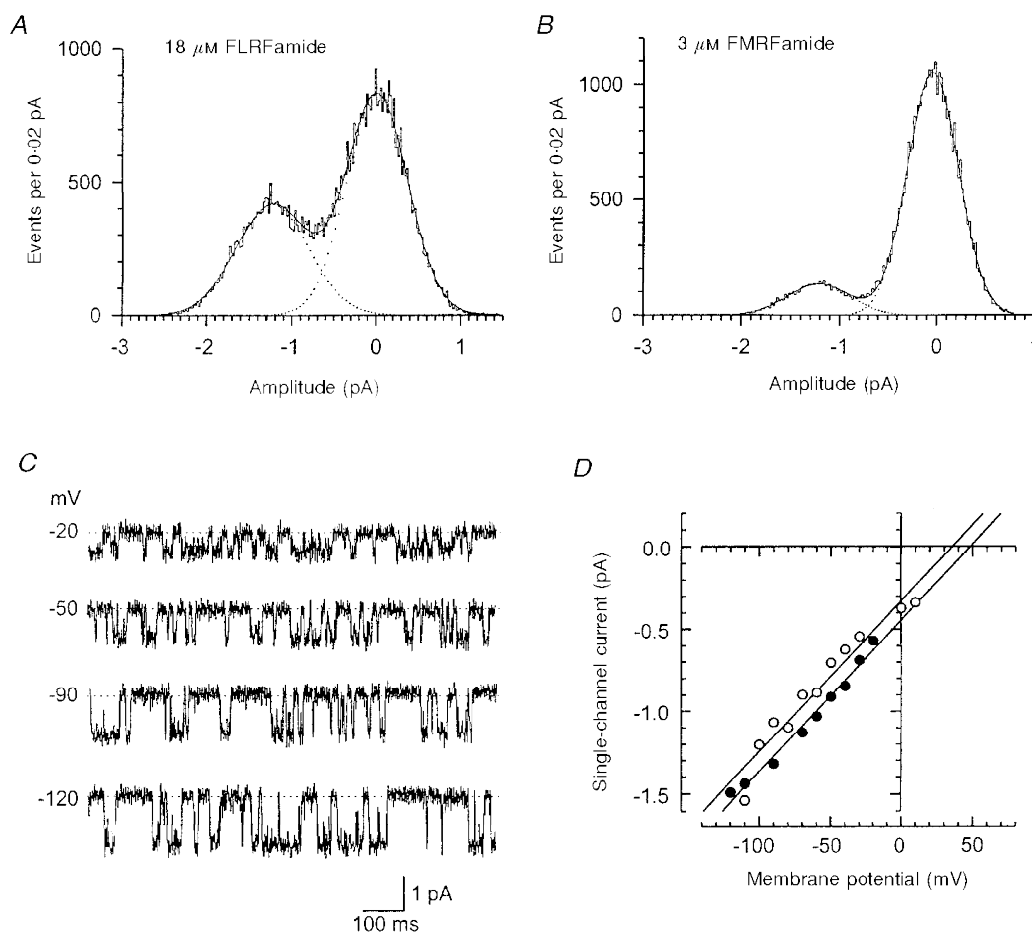


Figure 2. Current–voltage relation of the peptide-gated Na^+ channel

A and *B* are examples of histograms used to measure the amplitudes of unitary currents for each peptide (*A*, $18 \mu\text{M}$ FLRFamide; *B*, $3 \mu\text{M}$ FMRFamide). The histograms were fitted with the sum of two Gaussian components (continuous lines). The fit parameters had values of (mean (relative area)): $0.00 \pm 0.43 \text{ pA}$ (37%) and $1.24 \pm 0.36 \text{ pA}$ (63%) for FLRFamide, and $0.00 \pm 0.26 \text{ pA}$ (87%) and $1.18 \pm 0.32 \text{ pA}$ (13%) for FMRFamide. Examples of single-channel current traces at different membrane potentials (indicated to the left) are shown in *C*. The baseline is indicated by the dotted line. The outside-out patch was exposed to $1 \mu\text{M}$ FMRFamide and contained only one peptide-gated Na^+ channel. The traces were low-pass filtered at 320 Hz. The relationship between membrane potential and single-channel current amplitude for FMRFamide (●; $1 \mu\text{M}$) and FLRFamide (○; $1.8 \mu\text{M}$) is shown in *D* for each peptide. The data were taken from two patches. The slight displacement to the left of the FLRFamide-induced currents compared with those induced by FMRFamide most probably results from a difference in junction potential values, which were not corrected for with these two particular patches.

10 μM FLRFamide was applied to the extracellular surface of an outside-out patch of oocyte membrane.

Channel conductance

Amplitude histograms of the peptide-evoked unitary currents were fitted with the sum of two Gaussian components (Fig. 2*A* and *B*). At a membrane potential of -80 mV, the channel opened to a single level, which had an amplitude of -1.06 ± 0.11 pA ($N=7$) for 3 μM FMRFamide, and -1.17 ± 0.15 pA ($N=9$) for 18 μM FLRFamide. Figure 2*C* illustrates single-channel activity evoked by 1 μM FMRFamide at different membrane potentials (from -120

to -20 mV). The current–voltage relationship of the unitary current amplitude for each peptide is shown in Fig. 2*D*. The slope conductance between -120 and $+10$ mV was 9.2 pS for both FMRFamide and FLRFamide.

Concentration dependence of open probability and open channel current amplitude.

At low and moderate concentrations, the amplitude of the open channel current at -80 mV did not show any significant dependence on concentration for either of the peptides (Fig. 3*A*, *B* and *C*). However, at high concentrations (e.g. 100 μM for FMRFamide and 180 μM for FLRFamide),

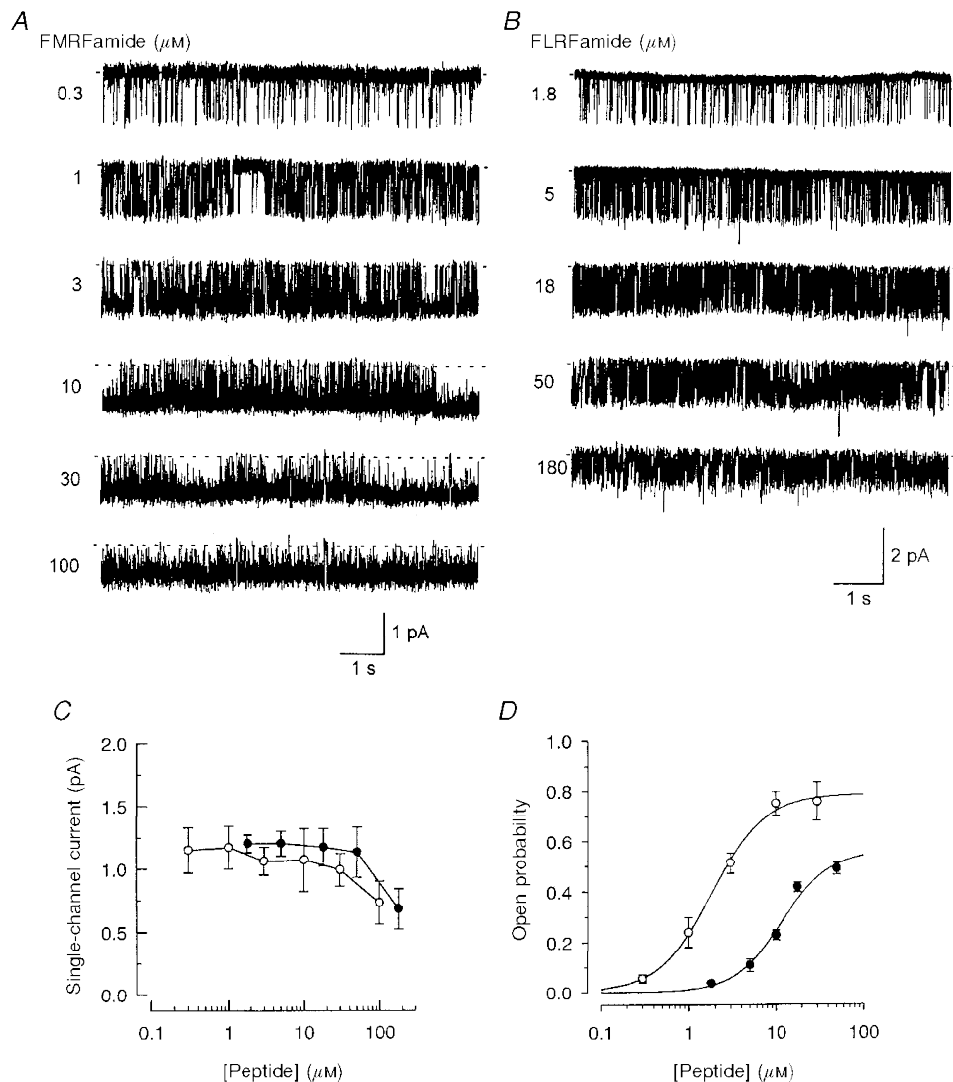


Figure 3. Dependence of channel activity on peptide concentration

Samples of peptide-gated unitary currents recorded at different concentrations of FMRFamide and FLRFamide are shown in *A* and *B*. Peptide concentrations are given near each trace. Baselines are depicted by dashed lines. The membrane potential was -80 mV and the recordings were low-pass filtered at 320 Hz (-3 dB). Traces in *A* and *B* are taken from two different patches. Each patch contained only one peptide-gated channel. The dependence of single-channel current amplitude on peptide concentration for each peptide (\circ , FMRFamide; \bullet , FLRFamide) is shown in *C*. Points are the mean \pm s.d. of 4–9 experiments. Note there is a marked reduction in unitary current amplitude at concentrations above 30 μM FMRFamide and 50 μM FLRFamide. In *D* the relationship between channel open probability and concentration of FMRFamide up to 30 μM (\circ) and FLRFamide up to 50 μM (\bullet) is shown for each peptide. The continuous lines show fits with the Hill equation (see text). Points shown are given as the mean \pm s.e.m. ($N=3-5$).

there was considerable increase in fast flickering between closed and open states (Fig. 3*A* and *B*). This led to an apparent decrease in open channel current amplitude (Fig. 3*C*); the fast transitions were brief compared with the rise time of the 2.0 kHz low-pass filter. Such fast flickerings most probably result from open channel blockade by the peptides. However, we did not attempt to investigate these effects further and limited our analysis of channel behaviour to the low and moderate agonist concentrations (0.3–30 μM for FMRFamide and 1.8–50 μM for FLRFamide).

Single-channel activity was increased in a dose-dependent manner as the FMRFamide concentration was increased from 0.3 to 30 μM (Fig. 3*A*). The open probability of the channel was increased from 0.06 ± 0.02 (s.e.m.; $N=4$) at 0.3 μM FMRFamide to 0.76 ± 0.08 (s.e.m.; $N=3$) at 30 μM FMRFamide (Fig. 3*D*). The open probability, P_o , could be fitted with the Hill equation:

$$P_o = P_{o,\max} C^n / (\text{EC}_{50}^n + C^n), \quad (1)$$

where C is the peptide concentration, $P_{o,\max}$ (0.79 ± 0.02 (s.e.m.)) is an asymptotic value of P_o , n (1.4 ± 0.1 (s.e.m.)) is the Hill coefficient, and EC_{50} (1.8 ± 0.1 (s.e.m.) μM) is the concentration for half-maximal effect. Similar behaviour was observed when the FLRFamide concentration was increased from 1.8 (P_o , 0.04 ± 0.01 (s.e.m.); $N=3$) to 50 μM (P_o , 0.49 ± 0.02 (s.e.m.); $N=5$) (Fig. 3*B*). The fit of the Hill equation to the data points gave the following parameters for FLRFamide (Fig. 3*D*): $P_{o,\max}$, 0.56 ± 0.08 (s.e.m.); n , 1.6 ± 0.3 (s.e.m.); EC_{50} , 11.7 ± 3.0 (s.e.m.) μM .

Dependence of single-channel kinetics on peptide concentration

Visual inspection of single-channel current recordings revealed two types of openings at low concentrations (e.g. 0.3 μM) of FMRFamide (Fig. 4). The first type was a brief single opening to the conducting level. The second type of opening generally occurred in groups, where such openings were separated by short closings. As the FMRFamide concentration was increased (to 1 or 3 μM), the occurrence of the brief single openings declined. At higher concentrations of FMRFamide (10 or 30 μM), groups of openings were dominant. FLRFamide-evoked single-channel activity was qualitatively similar to that evoked by FMRFamide, but at low FLRFamide concentrations the brief single openings were more numerous and durations of groups of openings were shorter than with FMRFamide (Fig. 5).

Distribution of open times

Distributions of channel open times were fitted with the sum of two exponential components. Figure 6*A* shows an example of the open time distribution in 0.3 μM FMRFamide, with open time constants (and relative areas) of $\tau_{o1} = 0.22$ ms (73%) and $\tau_{o2} = 4.46$ ms (27%). A similar two-component distribution of open times was obtained for 1.8 μM FLRFamide (Fig. 6*B*): $\tau_{o1} = 0.20$ ms (71%) and $\tau_{o2} = 2.77$ ms (29%). For both peptides, the open time constants did not show any obvious dependence on agonist concentration (Fig. 6*C*), but the relative area of the first component decreased, from $86 \pm 5\%$ ($N=5$) in 0.3 μM FMRFamide and $83 \pm 5\%$ ($N=5$) in 1.8 μM FLRFamide,

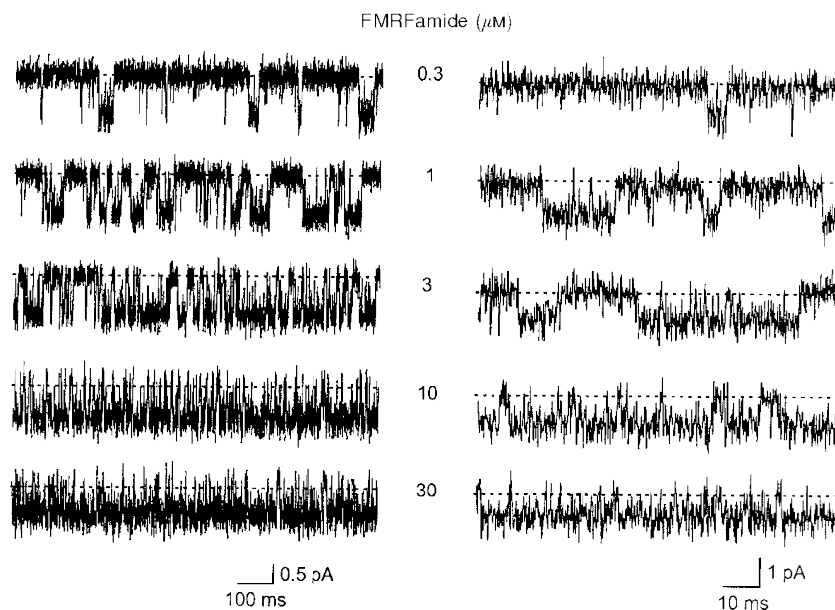


Figure 4. High-resolution samples of single peptide-gated channel activity at various concentrations of FMRFamide

The concentration of FMRFamide (0.3–30 μM) is shown near each current trace. In the right panel, the traces are shown on a more expanded time scale. Baselines are indicated by dashed lines. The membrane potential was -80 mV and the traces were low-pass filtered at 2 kHz (-3 dB). The patch contained only one peptide-gated Na^+ channel.

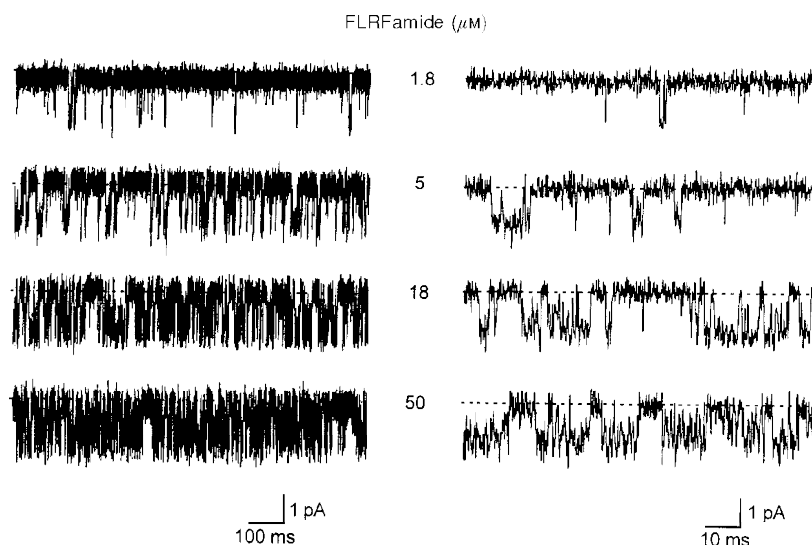


Figure 5. High-resolution samples of single peptide-gated channel activity at various concentrations of FLRFamide

The concentration of FLRFamide ($1.8\text{--}50\ \mu\text{M}$) is shown near each current trace. The traces are shown on a more expanded time scale in the right panel. Baselines are shown by dashed lines. The membrane potential was $-80\ \text{mV}$ and the traces were low-pass filtered at $2\ \text{kHz}$ ($-3\ \text{dB}$). The patch contained only one peptide-gated Na^+ channel.

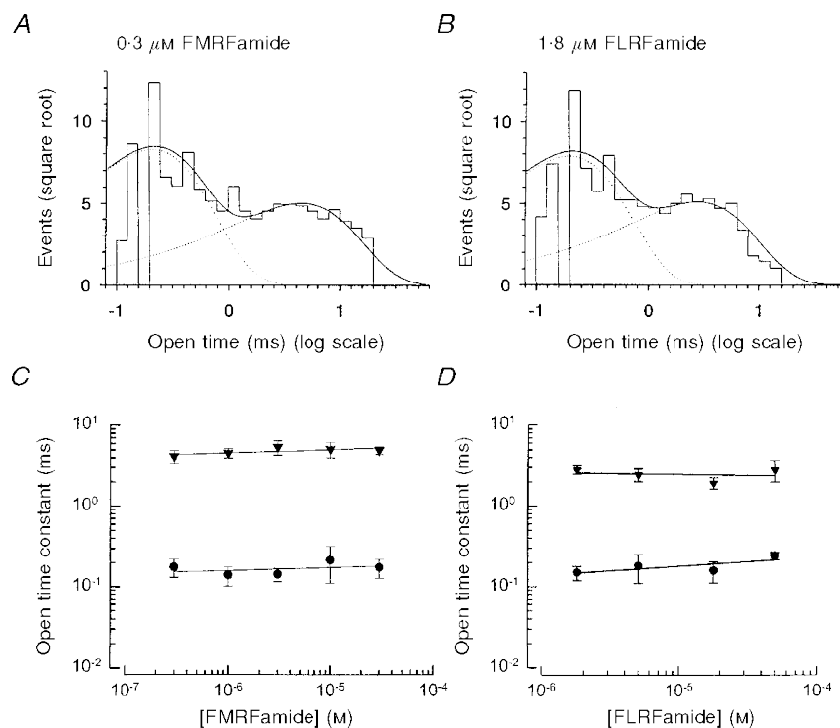


Figure 6. Distribution of open times

Distributions of open times of a single peptide-gated channel activated by FMRFamide (573 openings, $0.3\ \mu\text{M}$) and FLRFamide (511 openings, $1.8\ \mu\text{M}$) are shown in *A* and *B*. The distributions are fitted with the sum of two exponential components with parameters (mean time constant (relative area)) of: $0.22\ \text{ms}$ (73%) and $4.46\ \text{ms}$ (27%) for FMRFamide; $0.20\ \text{ms}$ (71%) and $2.77\ \text{ms}$ (29%) for FLRFamide. The mean open time constants are shown as a function of concentration for FMRFamide and FLRFamide in *C* and *D*. ● and ▼, first and second components of open time distributions, respectively. Continuous lines through the data points were drawn by hand. The membrane potential was $-80\ \text{mV}$ and the recording was low-pass filtered at $2\ \text{kHz}$ ($-3\ \text{dB}$). Points shown are the mean of 4 or 5 experiments.

to $18 \pm 10\%$ ($N=5$) in $10 \mu\text{M}$ FMRFamide and $36 \pm 28\%$ ($N=5$) in $18 \mu\text{M}$ FLRFamide. When open time constants were averaged over all peptide concentrations tested, it was found that the faster open time constant did not depend on agonist type ($\tau_{o1} = 0.17 \pm 0.03$ ms, $0.3\text{--}30 \mu\text{M}$ FMRFamide; $\tau_{o1} = 0.19 \pm 0.04$ ms, $1.8\text{--}50 \mu\text{M}$ FLRFamide), but the slower open time constant for FMRFamide was 1.9 times longer than for FLRFamide ($\tau_{o2} = 4.84 \pm 0.47$ ms, $0.3\text{--}30 \mu\text{M}$ FMRFamide); $\tau_{o2} = 2.59 \pm 0.42$ ms, $1.8\text{--}50 \mu\text{M}$ FLRFamide). Although the durations of channel openings were overestimated due to the presence of brief closings, which were not resolved by the recording system, it is likely that first and second components in the open time distribution correspond to single brief openings, and openings within groups, respectively (Figs 4 and 5).

Distribution of closed times

At all peptide concentrations tested, three exponential components were sufficient to fit the distributions of the closed times, suggesting that the channel has at least three closed states. Panels *A* and *B* in Figure 7 show examples of the distributions obtained in $0.3 \mu\text{M}$ FMRFamide and $1.8 \mu\text{M}$ FLRFamide, respectively. For each peptide the continuous line represents the fit of three exponentials with

parameters of (mean time constant (relative area)): 0.56 ms (33%), 7.13 ms (16%) and 88.7 ms (51%) with $0.3 \mu\text{M}$ FMRFamide, and 0.12 ms (30%), 2.43 ms (12%) and 35.4 ms (58%) with $1.8 \mu\text{M}$ FLRFamide. The fast component in the closed time distributions did not depend on peptide concentration (Fig. 7*C* and *D*). The averaged value of the fast closed time constant (τ_{c1}), over the range of peptide concentrations used, was 0.20 ± 0.03 ms for FMRFamide and 0.22 ± 0.04 ms for FLRFamide. The intermediate (τ_{c2}) and long (τ_{c3}) closed time constants (mean value (relative area)) decreased from 6.4 ± 0.7 ms (24%) and 77.4 ± 22.0 ms (27%) to 0.7 ± 0.3 ms (14%) and 3.4 ± 1.2 ms (10%), respectively, as the FMRFamide concentration was increased from 0.3 to $30 \mu\text{M}$ (Fig. 7*C*). Similar behaviour was observed for these two constants when the concentration of FLRFamide was increased (Fig. 7*D*), i.e. from $\tau_{c2} = 8.5 \pm 1.0$ ms (9%) and $\tau_{c3} = 60.3 \pm 21.8$ ms (48%) with $1.8 \mu\text{M}$ FLRFamide to $\tau_{c2} = 1.2 \pm 0.8$ ms (26%) and $\tau_{c3} = 8.4 \pm 3.1$ ms (26%) with $50 \mu\text{M}$ FLRFamide.

The long component (τ_{c3}) is likely to correspond to the long closed intervals separating adjacent single brief openings or group of openings (Figs 4 and 5). The openings inside the groups were typically interrupted by both brief and

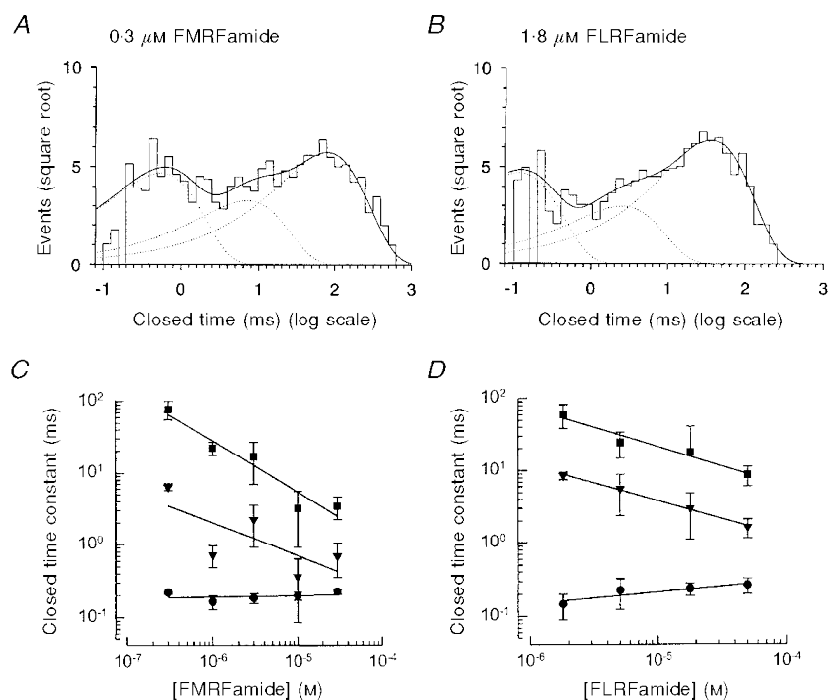


Figure 7. Distribution of all closed times

The distributions of all closed times of a single channel activated by FMRFamide (*A*; 593 closings, $0.3 \mu\text{M}$), and FLRFamide (*B*; 573 closings, $1.8 \mu\text{M}$) are shown. The distributions are fitted with the sum of three exponential components with parameters (mean time constant (relative area)) of 0.56 ms (33%), 7.13 ms (16%) and 88.7 ms (51%) for FMRFamide and 0.12 ms (30%), 2.43 ms (12%) and 35.4 ms (58%) for FLRFamide. The mean closed time constants are shown as a function of peptide concentration for FMRFamide (*C*) and FLRFamide (*D*). ●, ▼ and ■, first, second and third components of the closed time distributions, respectively. Continuous lines through the data points were drawn by hand. The membrane potential was -80 mV and the recording was low-pass filtered at 2 kHz (-3 dB). Points are given as the mean of 4 or 5 experiments.

intermediate closings, which presumably represent the fast and intermediate components in the closed time distributions.

Distribution of burst durations

The distribution of burst durations were best fitted by the sum of two exponential components. Figure 8A and B gives examples of the distribution of burst durations at 1.8 and 18 μM FLRFamide. The time constants of such distributions did not show any significant dependency on the concentration of FLRFamide (mean time constant (relative area)): $\tau_{\text{bf}} = 0.18 \pm 0.08$ ms (64%) and $\tau_{\text{bs}} = 7.3 \pm 3.0$ ms (36%) at 1.8 μM FLRFamide; $\tau_{\text{bf}} = 0.23 \pm 0.17$ ms (26%) and $\tau_{\text{bs}} = 6.0 \pm 1.6$ ms (74%) at 18 μM FLRFamide. At low concentrations of FLRFamide, the relative area of the fast component was larger than the slower component (Fig. 8A). When the FLRFamide concentration was increased, however, the relative area of the slower component became larger. In Fig. 8B, the ratio of the relative area of the slower component to that of the faster component (a_s/a_f) is shown as a function of FLRFamide concentration. The ratio increased linearly with the slope of $5.4 \times 10^4 \text{ M}^{-1}$ over the FLRFamide concentrations tested.

The same behaviour was observed for FMRFamide. The distributions of the burst durations were best fitted with the sum of two exponential components: $\tau_{\text{bf}} = 0.24 \pm 0.10$ ms

and $\tau_{\text{bs}} = 14.1 \pm 2.8$ ms at 0.3 μM FMRFamide; $\tau_{\text{bf}} = 0.18 \pm 0.16$ ms and $\tau_{\text{bs}} = 10.9 \pm 4.3$ ms at 30 μM FMRFamide. The ratio of the relative area of the slower component to one of the faster component (a_s/a_f) increased from 0.67 ± 0.03 at 0.3 μM FMRFamide to 1.72 ± 0.59 at 30 μM FMRFamide.

Very long bursts of openings

In some patches, the channel showed very long bursts of openings lasting from several to tens of seconds. A similar observation was made by Lingueglia *et al.* (1995). Such behaviour was observed with both peptides in the present study; it did not appear to be concentration dependent. Due to their very long duration and rare occurrence we have been unable to analyse these long bursts.

Distributions of open times within bursts and number of openings per burst

Although in general, open times within bursts are not distributed exponentially, their distributions could still be approximated with a sum of several exponential components (Colquhoun & Hawkes, 1982). Figure 9A shows examples of the distribution of open times within bursts fitted with the sum of two exponential components at three different concentrations of FMRFamide. The mean time constants did not show any obvious dependence on the peptide

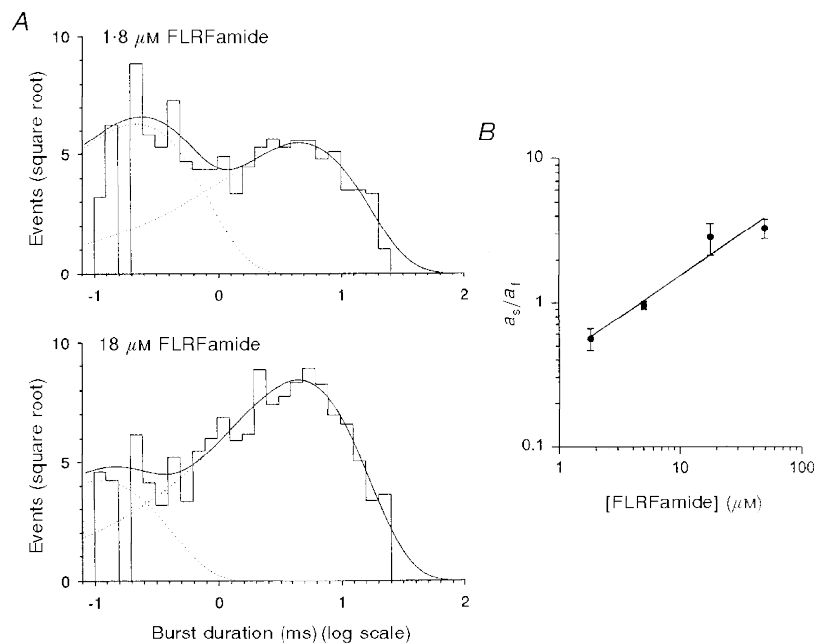


Figure 8. Distribution of burst durations

The distribution of burst durations of a single channel activated by FLRFamide is shown in A. In the top panel (1.8 μM FLRFamide), the sample contained 593 bursts and the critical interburst closed time (t_{crit}) was 3.06 ms. In the lower panel (18 μM FLRFamide), the sample comprised 886 bursts and the critical interburst closed time (t_{crit}) was 1.14 ms. The distributions were fitted with the sum (continuous lines) of two exponential components with parameters of (mean time constant (relative area)): 0.23 ms (57%) and 4.62 ms (43%) for 1.8 μM FLRFamide and 0.11 ms (20%) and 4.61 ms (80%) for 18 μM FLRFamide. The ratio of the relative area of the slower component to that of the faster component (a_s/a_f) is depicted as a function of FLRFamide concentration in B. The membrane potential was -80 mV and the recording was low-pass filtered at 2 kHz (-3 dB). Points are given as the mean \pm s.e.m. ($N = 4-5$).

concentration: 0.40 and 2.60 ms for 0.3 μM FMRFamide; 0.18 and 4.66 ms for 3.0 μM FMRFamide; 0.29 and 5.07 ms for 10 μM FMRFamide. However, the relative area of the faster component decreased from 59 to 5% as the FMRFamide concentration was increased from 0.3 to 10 μM (Fig. 9A).

It is likely that many of closings were missed due to the limited time resolution of the recording system. Nevertheless, the number of openings within bursts should still be distributed as a sum of several geometric components (Colquhoun & Sigworth, 1995). The number of channel open states are equal to the number of the components in the distribution of the number of openings within bursts. Examples of the distribution of the number of openings within bursts at three different concentrations of

FMRFamide are shown in Fig. 9B. The distributions were fitted with the sum of two geometrics according to the following equation (Colquhoun & Sigworth, 1995):

$$P(r) = a_1 \mu_1^{-1} (1 - \mu_1^{-1})^{r-1} + a_2 \mu_2^{-1} (1 - \mu_2^{-1})^{r-1}, \quad (2)$$

where a_1 and μ_1 are the area and mean value of the first component, a_2 and μ_2 are the area and mean value of the second component, and r is the number of openings. When the FMRFamide concentration was increased, the mean values of the distribution did not appear to change, but the relative contribution of the first component markedly decreased (mean value (relative area)): 1.25 ± 0.16 ($37 \pm 9\%$) and 2.95 ± 0.84 ($63 \pm 9\%$) in 0.3 μM FMRFamide; 1.05 ± 0.06 ($22 \pm 15\%$) and 2.81 ± 0.81 ($78 \pm 16\%$) in 1.0 μM FMRFamide; 1.01 ± 0.05 ($2 \pm 4\%$) and 3.82 ± 1.59

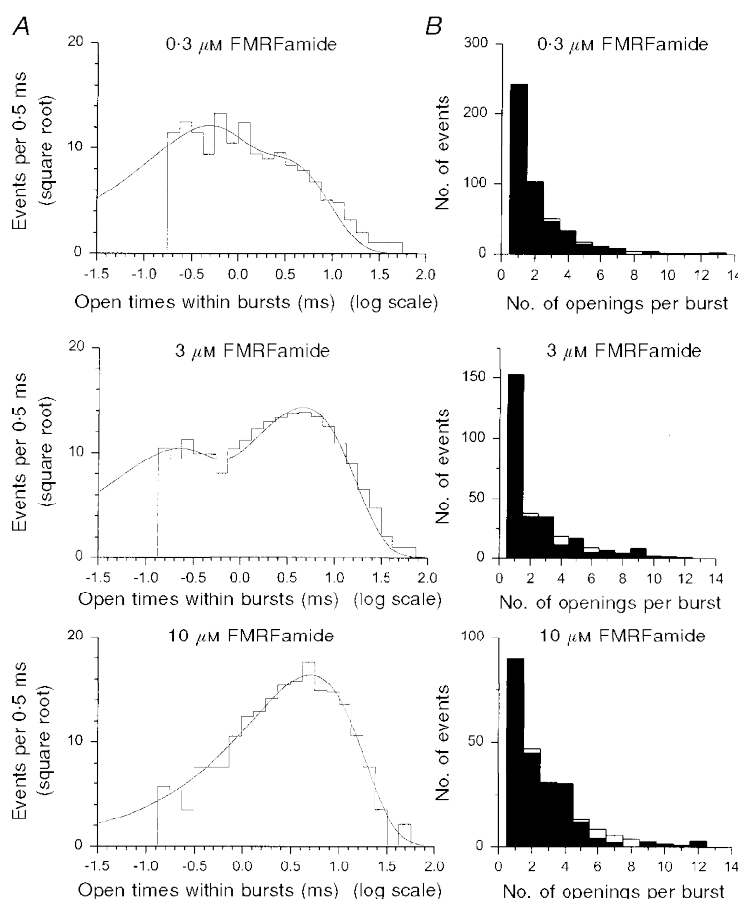


Figure 9. Distributions of open times within bursts and of the number of openings per burst

The distribution of open times within bursts with three concentrations of FMRFamide (top, 1534 openings, 0.3 μM ; middle, 2343 openings, 3 μM ; bottom, 610 openings, 10 μM) is shown in A. The critical interburst closed times were 13.79 ms for 0.3 μM , 1.94 ms for 3 μM , and 0.35 ms for 10 μM FMRFamide. The distribution was fitted with the sum of two exponential components (continuous lines) with parameters of (mean time constant (relative area)): 0.40 ms (59%) and 2.60 ms (41%) for 0.3 μM FMRFamide, 0.18 ms (30%) and 4.66 ms (70%) for 3.0 μM FMRFamide, and 0.29 ms (5%) and 5.07 ms (95%) for 10 μM FMRFamide. The membrane potential was -80 mV and the recording was low-pass filtered at 2 kHz (-3 dB). The distribution (filled bars) of the number of openings per burst at three concentrations of FMRFamide (top, 0.3 μM ; middle, 3 μM ; bottom, 10 μM) is shown in B. The distribution was fitted with the sum of two geometrics (open bars) with parameters of (mean number (relative area)): 1.4 (47%) and 2.9 (53%) for 0.3 μM FMRFamide, 1.1 (27%) and 2.7 (73%) for 3.0 μM FMRFamide, and 1.0 (8%) and 2.9 (92%) for 10 μM FMRFamide.

($98 \pm 4\%$) in $10 \mu\text{M}$ FMRFamide. Similar two-component distributions of the number of openings within bursts were obtained with FLRFamide (mean value (relative area)): 1.20 ± 0.30 ($91 \pm 14\%$) and 2.00 ± 0.07 ($10 \pm 14\%$) in $5 \mu\text{M}$ FLRFamide; 1.02 ± 0.04 ($5 \pm 6\%$) and 4.72 ± 1.95 ($95 \pm 6\%$) in $50 \mu\text{M}$ FLRFamide.

The first component with the mean value close to one most probably corresponds to the brief single openings seen in the single-channel current traces evoked by both peptides (Figs 4 and 5). At low peptide concentrations, the relative area of the first component was much larger for FLRFamide (91%) than for FMRFamide (37%), which probably reflects dominance of brief single openings in the FLRFamide-evoked single-channel activity. The second component can be ascribed to the group (or burst) of openings, although the mean value of the second component is certainly underestimated due to undetected brief closings.

Mean number of short closings per burst

There are three possible causes for the rapid closings observed within the long bursts. First, they may be caused by blockade of the channel by divalent cations. This is, however, unlikely because when the recordings were made in EGTA/EDTA buffered solutions with no added divalent cations, the channel still continued to show the brief closings among the longer openings. Secondly, they could result from open channel blockade by peptides. There was some indication that the open channel blockade by peptides does take place, but only in high peptide concentrations. Thirdly, the rapid flickerings might be an intrinsic property of the channel.

We looked to see whether the number of short closings within bursts depends on the peptide concentration. Short closings were counted and binned to give histograms. We defined short closings within bursts as closings shorter than a critical time interval (t_{crit}). The value of t_{crit} was calculated so that the number of long closed times within bursts (second component in all closed time distributions) that were misclassified as short closings within bursts was equal to the number of short closed times (first component in all closed time distributions) that were misclassified as long closed times within bursts. The distributions of the number of the short closings were fitted with one geometric. The mean

number of short closings did not depend on agonist concentration for either peptide (Fig. 10). The averaged number of short closings (n_{sc}) over the peptide concentrations tested were 1.48 ± 0.10 for FMRFamide and 1.18 ± 0.03 for FLRFamide. The lack of dependence of rapid flickerings inside bursts on the agonist concentration suggests that these short closings do not result from rapid binding and unbinding of peptides to the channel. It is likely therefore that they represent an intrinsic property of the channel, although we cannot exclude completely the possibility that these rapid flickerings come from open channel blockade by agents other than divalent cations and peptides.

DISCUSSION

Single-channel conductance and dose–response relationship

The peptides FMRFamide and FLRFamide activated unitary currents in *Xenopus* oocytes injected with cRNA prepared from the *Helix aspersa* clone FaNaCh. The data and analyses reported here confirm and extend the findings of Lingueglia *et al.* (1995). These workers made both whole-oocyte and patch recordings. EC_{50} values obtained using two-electrode voltage clamp for FMRFamide and FLRFamide were respectively 2 and $11 \mu\text{M}$ (Lingueglia *et al.* 1995), very similar to the values of 1.8 and $11.7 \mu\text{M}$ obtained in the present study with unitary current recordings. Lingueglia *et al.* (1995) also noted, using two-electrode voltage clamp, that activation by FMRFamide and FLRFamide was co-operative with an apparent Hill coefficient of 1.6. In a similar series of experiments, evidence for co-operativity was obtained for FMRFamide, FLRFamide and the synthetic peptide FnorLRFamide; apparent Hill coefficients ranged from 1.4 to 1.7 (Cottrell 1997).

The unitary current recordings of Lingueglia *et al.* (1995), most of which were made using the cell-attached configuration, yielded a slope conductance of 13.1 pS. Using $30 \mu\text{M}$ FMRFamide and a cut-off frequency of 1 kHz, they reported one exponential open time distribution (4 ms) and two exponential closed time distributions (8 and 30 ms); the reason why the fast open, and closed, time components reported in the present study were not detected is probably due to the low cut-off frequency used. The slope

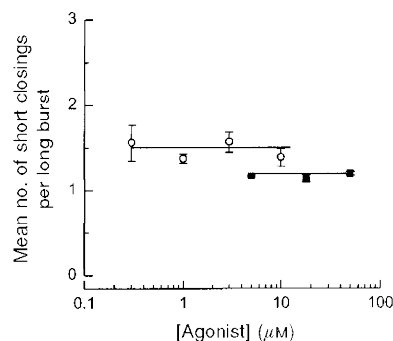


Figure 10. The mean number of short closings within long bursts at various concentrations of peptide

○, FMRFamide; ■, FLRFamide. Continuous lines through the data points were drawn by hand. The points shown are given as the mean of 4–5 experiments.

conductance of the unitary currents was 13·1 pS, similar though not identical to the value of 9·2 pS obtained in the present work. Both of these values are, however, much higher than the value of 4·1 pS, obtained with isolated outside-out patches taken from *Helix aspersa* neurones, in which the channel was first detected (Cottrell *et al.* 1990).

In our experiments, both FMRFamide and FLRFamide at high concentrations (i.e. close to, or higher than, those concentrations required to produced maximum responses in intact oocytes; see Lingueglia *et al.* 1995; Cottrell 1997) evoked fast flickering between open and closed states of the channel and an apparent decrease in channel current amplitude. This phenomenon restricted our analysis to low and moderate peptide concentrations. Even with such a limited concentration range the data suggest that for each peptide channel open probability P_o is dependent on peptide concentration with the Hill coefficient of about 1·5, similar to previous findings using two-electrode voltage clamp (see above). Thus all the available results suggest that binding of at least two peptide molecules is required for full channel activation.

Number of closed and open states of the channel

The number of components required to fit the distribution of open times, the distribution of burst durations, and the distribution of number of openings within bursts, i.e. 2, indicates that there are at least two open states. The mean open time for each open state was not dependent on peptide concentration, but the longer open time was 1·9 times greater for FMRFamide than for FLRFamide. Lingueglia *et al.* (1995) only reported patch clamp data with FMRFamide (30 μM). Filtering at 1 kHz, they reported an open time distribution ($\tau_o = 4$), which is similar to the second component of the open time distribution reported here ($\tau_{o2} = 4\cdot84$).

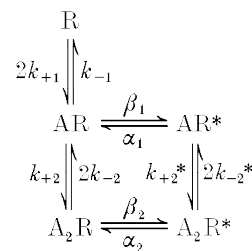
We ascribe the origin of the brief single openings, which corresponds to the faster component in the distribution of open times detected in our data, to openings of the channel with only one ligand molecule bound (as in Colquhoun & Sakmann, 1985). Consequently, openings within bursts, which corresponds to the slower component in the distribution of open times, can be ascribed to openings of the fully liganded channel. The following observations support this interpretation: (1) current amplitudes of both openings were quite similar; (2) the ratio of the relative area of the slower component to one of the faster component in the distribution of burst durations increased linearly with peptide concentration.

Three exponential components were needed to fit the distribution of all closed times, indicating that the channel has at least three closed states. The states could be ascribed to the unliganded channel and the channel liganded (but closed) with one or two peptide molecules. There may be additional states corresponding to open channel blockade by the peptides seen at very high peptide concentrations, but this possibility has not been explored here. As the peptide

concentration was increased, the long and intermediate mean closed times, which are likely to correspond to lifetimes of unliganded and single-liganded closed states, decreased, indicating that transitions from these states involve the binding of peptide. The shortest mean closed time, corresponding to the brief closings within bursts, did not depend on peptide concentration. Thus such brief closings are unlikely to be due to open channel blockade by the peptide itself. It is likely that they result from rapid transitions between the fully liganded closed and open states.

Interpretation of the data in terms of a five-state model

The likely existence of two open and three closed states of the channel in the presence of the natural ligand(s) is similar to the channel states observed by Colquhoun & Sakmann, (1985) for the nicotinic ACh receptor of the frog neuromuscular junction. We have therefore used a similar approach and similar assumptions to these workers to interpret our data. The scheme for the ligand binding and activation of the channel is shown below:



Scheme 1

R, AR, A₂R represent unliganded, single-liganded and double-liganded closed states, respectively, while AR* and A₂R* are open states of the channel with one and two peptide molecules bound, respectively. The absence of the form R* in the scheme reflects the fact that the unliganded channel was not observed to open in the absence of the peptides.

In this scheme, groups (or long bursts) of openings would occur by multiple transitions of the channel between the states AR, A₂R and A₂R* before entering state R. Short closings within bursts are caused by rapid transitions between A₂R and A₂R* and transitions between AR, and AR* correspond to brief single openings.

The mean open times of brief single openings and openings within long bursts are therefore given by the following equations:

$$\tau_{o1} = 1/(\alpha_1 + k_{+2}^* C), \tag{3}$$

$$\tau_{o2} = 1/(\alpha_2 + 2k_{-2}^*), \tag{4}$$

where C is a peptide concentration. In our experiments, the mean open time of single-liganded open state was not dependent on peptide concentration, indicating that transitions between the two open states are very rare and may be omitted from the scheme. Equations (3) and (4)

Table 1. Estimated rate constants for the five-state model shown above

	k_{+1}, k_{+2} ($\text{M}^{-1} \text{s}^{-1}$)	k_{-1} (s^{-1})	k_{-2} (s^{-1})	β_1 (s^{-1})	β_2 (s^{-1})	α_1 (s^{-1})	α_2 (s^{-1})
FMRFamide	1.225×10^8	100	1010	10	2980	5882	207
FLRFamide	2.300×10^7	40	1040	5	2460	5260	386

therefore allow us to estimate the values of α_1 and α_2 , which give the following values: $\alpha_1 = 1/\tau_{o1} = 5882 \text{ s}^{-1}$ and $\alpha_2 = 1/\tau_{o2} = 207 \text{ s}^{-1}$ for FMRFamide.

The mean short closed time, τ_{c1} , and the mean number of short closings within bursts, n_{sc} , would also be given by the following equations:

$$\tau_{c1} = 1/(\beta_2 + 2k_{-2}), \quad (5)$$

$$n_{sc} = \beta_2/(2k_{-2}), \quad (6)$$

For FMRFamide, eqns (5) and (6) give estimates of $k_{-2} = 1010 \text{ s}^{-1}$ and $\beta_2 = 2980 \text{ s}^{-1}$.

As the closed states all intercommunicate, allowance must be made for the possibility of invisible oscillations between them, especially between states A and AR. To estimate the transition rate constants between the closed states, we used standard Q-matrix procedures (see e.g. Colquhoun & Hawkes, 1982) to compute the probability of observing each experimental dwell time given a set of trial rate constants, including those estimated more directly above. In the absence of evidence to the contrary, we have made the assumption that $k_{+2} = k_{+1}$, i.e. that the peptide binds equally well to each of the proposed sites of interaction. Estimates made in this way for the transition rate constants for each peptide are shown in Table 1.

Notable differences between the peptides are the binding constants (k_{+1} and k_{+2}), which are 5- to 6-fold greater for FMRFamide than FLRFamide, and the rate constant for closure of the longer open state (α_2), which is almost twice as large for FLRFamide as for FMRFamide. There are also approximately 2-fold differences in the constants β_1 and k_{-1} .

Conclusions

The pattern of openings and closings evoked by the peptide agonists of this unusual type of ligand-gated channel conform well to the model proposed for the nicotinic ACh receptor. Thus, the five-state model also provides a plausible mechanism to account for the unitary current activity of this peptide-gated Na^+ channel. A limitation of our study has been the relatively poor resolution of very fast events, compared with those achieved in the study of Colquhoun & Sakmann (1985). Nevertheless, even at the level of analysis achieved, a similar view emerges of ligand binding and slower onset 'isomerization' of the channel with intermittent fast closings. Thus, it would appear that receptors as

dissimilar as the nicotinic ACh channel and the FMRFamide Na^+ channel can behave similarly in response to activation by their natural ligands.

The higher apparent affinity of the channel for FMRFamide than for FLRFamide, observed in earlier studies, relates to the differences in the rate constants k_{+1} and k_{+2} for FMRFamide ($1.225 \times 10^8 \text{ M}^{-1} \text{ s}^{-1}$) and FLRFamide ($2.30 \times 10^7 \text{ M}^{-1} \text{ s}^{-1}$). The data also suggest that the larger maximum response at high peptide concentrations observed with FMRFamide compared with FLRFamide, in both the heterologously expressed channel and the neuronal channel (see Cottrell, 1997), results mainly from differences in the rate constants α_2 and β_2 for FMRFamide (207 and 2980 s^{-1}) and FLRFamide (386 and 2460 s^{-1}).

At high concentrations of both peptides, the channel would behave as a two-state channel undergoing rapid transitions between states A_2R and A_2R^* , and the open probability would be given by the expression $\beta_2/(\alpha_2 + \beta_2)$. Using values of α_2 and β_2 for each peptide, one can estimate the ratio of the maximum response for FLRFamide relative to that for FMRFamide, which equals 0.9. This value is slightly larger than that determined experimentally, which was 0.7. Both of these values are, however, greater than the ratio of the maximum responses to the two peptides observed with whole oocytes, which was about 0.6. Very high concentrations of the peptides were used to complete the dose-response curves in the whole-oocyte experiments. In the light of the single-channel data, it now seems likely that open channel block by the very high FLRFamide concentrations, in addition to the differences in the rate constants α_2 and β_2 , could contribute to the large difference observed in the whole-cell experiments.

CANESSA, C. M., HORISBERGER, J.-D. & ROSSIER, B. C. (1993). Epithelial sodium channels related to proteins involved in neurodegeneration. *Nature* **361**, 467-470.

CANESSA, C. M., SCHILD, L., BUELL, G., THORENS, B., GAUTSCHI, I., HORISBERGER, J.-D. & ROSSIER, B. C. (1994). Amiloride-sensitive epithelial Na channel is made up of three homologous subunits. *Nature* **367**, 463-467.

COLOMBAIONI, L., PAUPARDIN-TRITSCH, D., VIDAL, P. P. & GERSCHENFELD, H. M. (1985). The neuropeptide FMRF-amide decreases both the Ca^{2+} conductance and a cyclic 3',5'-adenosine monophosphate-dependent K^+ conductance in identified molluscan neurones. *Journal of Neuroscience* **5**, 2533-2538.

- COLQUHOUN, D. & HAWKES, A. G. (1982). On the stochastic properties of bursts of single ion channel openings, and of clusters of bursts. *Philosophical Transactions of the Royal Society B* **300**, 1–59.
- COLQUHOUN, D. & SAKMANN, B. (1985). Fast events in single-channel currents activated by acetylcholine and its analogues in the frog muscle end-plate. *Journal of Physiology* **369**, 501–557.
- COLQUHOUN, D. & SIGWORTH, F. J. (1995). Fitting and statistical analysis of single-channel records. In *Single-Channel Recording*, ed. SAKMANN, B. & NEHER, E., pp. 483–633. Plenum Press, New York.
- COTTRELL, G. A. (1997). The first peptide-gated ion channel. *Journal of Experimental Biology* **200**, 2377–2386.
- COTTRELL, G. A. & DAVIES, N. W. (1987). Multiple receptors for a molluscan peptide (FMRFamide) and related peptides in *Helix*. *Journal of Physiology* **382**, 51–68.
- COTTRELL, G. A., DAVIES, N. W. & GREEN, K. A. (1984). Multiple actions of a molluscan cardio-excitatory neuropeptide and related peptides on identified *Helix* neurones. *Journal of Physiology* **356**, 315–333.
- COTTRELL, G. A., GREEN, K. A. & DAVIES, N. W. (1990). The neuropeptide Phe-Met-Arg-Phe-NH₂ (FMRFamide) can activate a ligand-gated ion channel in *Helix* neurones. *Pflügers Archiv* **416**, 612–614.
- DRISCOLL, M. & CHALFIE, M. (1992). Developmental and abnormal cell death in *C. elegans*. *Trends in Neurosciences* **15**, 15–19.
- GREEN, K. A., FALCONER, S. W. P. & COTTRELL, G. A. (1994). The neuropeptide Phe-Met-Arg-Phe-NH₂ directly gates two ion channels in an identified *Helix* neurone. *Pflügers Archiv* **428**, 232–240.
- GREENBERG, M. J. & PRICE, D. A. (1992). The relationships among the FMRFamide-like peptides. *Progress in Brain Research* **92**, 25–37.
- HAMILL, O. P., MARTY, A., NEHER, E., SAKMANN, B. & SIGWORTH, F. J. (1981). Improved patch-clamp techniques for high resolution current recording from cells and cell-free membrane patches. *Pflügers Archiv* **391**, 85–100.
- HUANG, M. & CHALFIE, M. (1994). Gene interactions affecting mechanosensory transduction in *Caenorhabditis elegans*. *Nature* **367**, 467–470.
- LINGUEGLIA, E., CHAMPIGNY, G., LAZDUNSKI, M. & BARBRY, P. (1995). Cloning of the amiloride-sensitive FMRFamide peptide-gated sodium channel. *Nature* **378**, 730–733.
- LINGUEGLIA, E., VOILLEY, N., WALDMANN, R., LAZDUNSKI, M. & BARBRY, P. (1993). Expression cloning of an epithelial amiloride-sensitive Na⁺ channel. A new channel type with homologies to *Caenorhabditis elegans* degenerins. *FEBS Letters* **318**, 95–99.
- LUTZ, E. M., MACDONALD, M., HETTLE, S., PRICE, D. A., COTTRELL, G. A. & SOMMERVILLE, J. (1992). Structure of cDNA clones and genomic DNA encoding FMRFamide-related peptides (FaRPs) in *Helix*. *Molecular and Cellular Neuroscience* **3**, 373–382.
- PRESS, W. H., TEUKOLSKY, S. A., VETTERLING, W. T. & FLANNERY, B. P. (1992). *Numerical Recipes*, 2nd edn. Cambridge University Press, Cambridge.
- PRICE, D. A., DOBLE, K. E., LESSER, W., GREENBERG, M. J., SWIDEREK, K. M., LEE, T. D., LUTZ, E. M., SOMMERVILLE, S., FALCONER, S. & COTTRELL, G. A. (1996). The peptide pQFYRFamide is encoded on the FMRFamide precursor of the snail *Helix aspersa* but does not activate the FMRFamide-gated sodium current. *Biological Bulletin* **191**, 341–351.
- WALDMANN, R., BASSILANA, F., DE WEILLE, J., CHAMPIGNY, G., HOURTEAUX, C. & LAZDUNSKI, M. (1997a). Molecular cloning of a non-inactivating proton-gated Na⁺ channel specific for sensory neurons. *Journal of Biochemistry* **272**, 20975–20978.
- WALDMANN, R., CHAMPIGNY, G., BASSILANA, F., HOURTEAUX, C. & LAZDUNSKI, M. (1997b). A proton-gated cation channel involved in acid sensing. *Nature* **386**, 173–177.

Acknowledgements

We thank Professor David Colquhoun of the Department of Pharmacology, University College London, UK, for informative discussions and making available the Q-matrix software, Ms L. Milstead for help with the illustrations and The Wellcome Trust and the National Institute on Deafness and Other Communication Disorders (DC 01655) for providing financial support.

Corresponding author

G. A. Cottrell: School of Biomedical Sciences, University of St Andrews, Bute Medical Building, St Andrews, Fife KY16 9TS, UK.

Email: gac@st-andrews.ac.uk and cottrell@mail1.aug.com